Density maps of the herring gull for the Dutch continental shelf

Memo to supplement the seabird assessment reports within KEC ("Kader Ecologie en Cumulatie") 4.0

Author(s): F.H. Soudijn[1], C. Chen[1], A. Potiek[2], S. van Donk[1]

[1] Wageningen Marine Research
[2] Bureau Waardenburg

WAGENINGEN
UNIVERSITY & RESEARCH

This report can be downloaded for free from https://doi.org/10.18174/566013
Wageningen Marine Research provides no printed copies of reports

Wageningen Marine Research is ISO 9001:2015 certified.

Disclaimer
In deze rapporten is gewerkt met de LNV-werknormen voor de ALI. Deze zijn op het moment van vaststellen van dit rapport nog niet definitief. Mochten de werknormen eventueel wijzigen dan heeft dit geen invloed op de in dit rapport beschreven methodiek en slachtofferberekeningen. Mochten de werknormen wijzigen dan zullen tabel 5.1 (rapport Cumulative impact assessment of collisions with existing and planned offshore wind turbines in the southern North Sea Analysis of additional mortality using collision rate modelling and impact assessment based on population modelling for the KEC 4.0) en tabel 10 (rapport Cumulative impact assessment of collisions with existing and planned offshore wind turbines in the southern North Sea Analysis of additional mortality using collision rate modelling and impact assessment based on population modelling for the KEC 4.0) aangepast worden.

Contents

Publiekssamenvatting

Dit document is een oplegnotitie bij de KEC 4.0 assessment rapporten van de effecten op zeevogelpopulaties van aanvaringen met (Potiek *et al.* 2022) en habitatverlies door (Soudijn *et al.* 2022) offshore windmolenparken. Het werk dat hier wordt beschreven bouwt voort op de methodiek die wordt beschreven in deze rapporten en kan niet onafhankelijk worden beschouwd van deze rapporten. Vanwege onzekerheden in de dichtheidskaarten die werden gebruikt in KEC 4.0, is een verkennende analyse gedaan voor mogelijke verbetering van de dichtheidskaarten van de zilvermeeuw. Er zijn zilvermeeuwkaarten gemaakt met vijf verschillende methodes. De kaarten gebaseerd op het regressiemodel met de variabelen afstand tot de kust, visserij activiteit en waterdiepte lijkt de verdeling van zilvermeeuwen het beste te voorspellen. Op deze kaarten is de typisch kust gebonden verdeling van de zilvermeeuwen duidelijk terug te zien. Het regressiemodel dat we hebben ontworpen kan omgaan met datasets die een hoog percentage nul waarnemingen ("zero-inflated" data) en grote variabiliteit in waarnemingen, van met name de hoge dichtheden, hebben, zoals vaak voorkomt bij meeuwen op zee. De populatie-effecten van aanvaringen met windmolenparken die worden voorspeld gebaseerd op de nieuwe kaarten (gebaseerd op het regressiemodel) overschrijden de 'Acceptable Levels of Impact' (ALIs) voor alle nationale scenario's (zie voor een definitie van de scenario's Potiek *et al.* 2022). De sterftekans door aanvaringen is iets lager op basis van de nieuwe vergeleken met de oude kaarten. Vanwege de hoge tijdsdruk binnen dit project moeten de dichtheidskaarten als voorlopige kaarten worden beschouwd. In verder onderzoek moet modelselectie worden uitgevoerd om de meest geschikte covariabelen te ontdekken om de verspreiding van zilvermeeuwen te verklaren en voorspellen. Verder moet een betere proxy voor visserijactiviteit worden ontwikkeld. Daarnaast, moeten de door het regressiemodel geschatte onzekerheidsintervallen in de dichtheden worden gebruikt om onzekerheden aan te geven in de uitkomsten van de schattingen van slachtoffers en effecten op populatieniveau. Ten slotte is extra werk nodig om de voorspellingen van het ruimtelijke model te vergelijken met veldobservaties, en het voorspellend vermogen van het model te bepalen.

Summary

This document is a memo that is written as an addition to the KEC 4.0 assessment reports of the effects of collision risk (Potiek *et al.* 2022) and habitat loss (Soudijn *et al.* 2022) from offshore windfarms on seabird populations. It relies heavily on the methodology described in these reports and cannot be considered independently from these reports. Because of uncertainties in the density maps of the herring gull as used in the KEC 4.0 assessment, exploratory analyses were conducted to improve the maps. New national density maps were created based on five methods and were compared with the original herring gull density maps from KEC 4.0. The density maps based on predictions of a regression model with the covariates distance to coast, fishing intensity and water depth as predictors seem to represent the natural (mainly coastal) distribution of the herring gull the best. Regression models are capable of handling data with many zero observations ("zero-inflated" data) and high variability in observations of especially high bird densities, which is typical for the herring gulls at sea. Based on the original maps and the maps newly developed here, the estimated population-level effects of collision mortality exceed the ALIs for all national scenarios. Yet, the estimated collision mortality was found to be slightly lower with the new density maps based on the regression model. Due to the strong time constraints of the project, the newly developed density maps need to be considered as preliminary. Future research should focus on model selection to tease out the most appropriate covariates to predict the herring gull distribution and developing a better proxy for fishing activity. In addition, the confidence intervals estimated in the densities by the regression model should be used to indicate uncertainties in the outcomes of the casualty estimations and population-level effects. Finally, rigorous testing of the performance of the model (through a comparison of model predictions with field observations) should be conducted in order to determine its predictive power.

1 Assignment

In the coming decades, new areas of the North Sea will be appointed for wind energy development. Offshore wind farms (OWFs) form an important pillar of the Dutch renewable energy strategy and in the programme 'Programma Noordzee 2022-2027' additional wind energy search areas are planned in the North Sea. The potential ecological effects of the development of these areas on seabirds are assessed with the 'Kader Ecologie en Cumulatie' (KEC) framework. This memo is written as part of the latest KEC assessment, KEC 4.0 (Potiek *et al.* 2022, Soudijn *et al.* 2022).

In KEC 4.0, adverse effects of habitat loss due to OWFs and collisions in OWFs were assessed on seabird populations. During the latest assessment, it became obvious that some of the components of the assessment framework contain high uncertainties. It was therefore decided to do some additional exploratory analyses. Here, we compare different approaches to predict density maps of the herring gull (*Larus argentatus*). The herring gull was chosen as the target species because the density maps that were originally predicted for this species showed some unexpected patterns, that were thought to not represent the actual distribution of the birds. While the herring gull is a coastally oriented species (van Donk *et al.,* 2019, Vanermen *et al.,* 2020), the original maps predicted relatively high densities of herring gull further away from the coast.

The original KEC method is based on density maps that are calculated using 'inverse-distance-weighing' (IDW). This technique calculates mean values per grid cell based on a defined number of values in the grid cells within a predefined radius around the grid cell. Bird observational data is typically 'zero-inflated' data, meaning that observations of birds are relatively rare and the dataset contains many zero values. Moreover, when birds are present they sometimes occur in high densities. This is especially true for species such as herring gull, that tend to gather behind fishing vessels. To deal with such disbalances in observations, high densities were spread out in squares of 11 x 11 grid cells prior to the IDW calculation in the original KEC assessment method. The high density observations are highly variable in space and time but the chance of encountering them in each location is very low. Such disbalances in observational data are difficult to deal with, but certain spatial regression models are capable of reliable mean density predictions even with such high variability in observational data.

The analysis that we performed for the herring gull density maps contains the following variants:
1. IDW density maps based on the raw data, without spreading out of the high density observations.
2. IDW density maps based on data in which high densities were spread out using kernels instead of squares.
3. Kriging density maps with covariate distance to coast.
4. Density maps based on predictions of INLA Spatial regression model of herring gull density with the covariates distance to coast, fishing activity and water depth.

For each technique that was used, six maps were produced, one for each two-month period of the year. We did visual inspections of the maps to determine which method resulted in density maps that gave the best representation of the herring gull distribution and compared the total densities predicted by each of the methods. Using the density maps based on the predictions of the INLA regression model, the number of casualties of collisions with OWFs were predicted with the methods described in the main KEC 4.0 report (Potiek *et al.* 2022). Subsequently, the population-level effects of the collisions were predicted using the population models described in the main KEC 4.0 report (Potiek *et al.* 2022).

There was little time to complete the additional analyses of the density maps because the KEC 4.0 assessment is used for current political advice regarding the designation of search areas for the development of wind energy. To stay within the time limits set by the commissioner (RWS), several

simplifications were necessary in the INLA spatial regression model step: 1. We chose covariates for which the information was readily available to us, 2. We did not perform a model selection procedure, 3. We did not perform model performance tests.

2 Materials and Methods

2.1 Data selection

The dataset used was identical to the dataset used for the density maps in the main KEC 4.0 report (Soudijn *et al.* 2022). The grid used for all interpolations has a resolution of 5x5 km. We made maps for the national scenarios only, which were based on data from the MWTL counted at the NCP after 2000 (see Soudijn *et al.,* 2022). After the data selection and preprocessing (Soudijn *et al.* 2022), mean densities were take per grid cell per two-month period per year, except for the kriging method and the INLA modelling, where raw data were used as an input. We describe each of the methods to produce new maps in detail in the sections below. The methods fall broadly into three categories: IDW maps, kriging maps and INLA regression maps.

As a measure of fishing intensity, the monthly number of fishing hours per grid cell were derived from bottom trawl fisheries in the North Sea as collated by ICES. This data covers the time period from 2010-2018. Since we would like to include fishing intensity as a covariate in the model, only 2010-2018 MWTL bird data were used in the model fit. Also the prediction map was based on the fishing intensity data from 2010-2018. Additional covariates in the model included distance to coast and water depth.

2.2 Inverse distance weighting

Inverse distance weighting (IDW) is an interpolation method whereby average values are calculated for each grid cell based on a set of values in the grid cell itself and the values in the grid cells around the grid cell. The method of interpolation used was based on the method previously described in Leopold *et al.,* (2014) and van der Wal *et al.,* (2019). IDW was conducted using R (R Core Team 2014) and the R-package "gstat". Each value was based on a minimum of 5 and a maximum of 15 values, the maximum distance over which values were included was 317 km. The inverse distance weighting power was set to 2. We interpolated using IDW based on: a. the raw data and b. a dataset in which high densities were spread out using a Gaussian kernel.

For map type b, all observations of densities higher than 10 gulls/km^2 were spread out. The spreading out was conducted based on the idea that herring gulls are attracted by fishing vessels and are naturally expected to be distributed more broadly in space. Where the previous method spread the values over squared areas of 11x11 grid cells (55x55 km)(see Leopold *et al.,* 2014, van der Wal *et al.,* 2018), we used a gaussian kernel to spread out the values, with a band width of 25 km. This means, in practice, that the values were spread out over an area of about 10x10 grid cells (50x50 km).

2.3 Kriging

Kriging is a type of distance weighed interpolation, in which covariates can be used to estimate the best linear unbiased local value. Kriging cannot be performed when coordinates of observations overlap. This happens when more observations are done at the same location. Therefore, overlapping coordinates where slightly changed by adding or subtracting 5-50m to the y coordinate. The kriging was done using R (R Core Team 2014) and the R package "automap". Kriging was performed with the covariate distance to coast, and with the covariates distance to coast and fishing effort.

2.4　INLA regression model

The regression method assumes that herring gull density at every spatial location follows a statistical distribution. The mean value of such distributions is associated with some known factors such as distance to coast or fishing intensity, while the causes of the residual spread around the mean values are unknown. The regression method aids in explaining the underlying mechanisms causing the herring gull density distribution, and as a result, it allows identifying "true" hotspots, where high densities are caused by short distances to the coast or high fishing activity. Another advantage of the regression method is that it provides uncertainty around the estimated densities. Moreover, the regression method can handle unbalanced spatial coverage in observations.

Model structures
The density distribution of herring gulls are highly 'zero-inflated': 95% of the observations are zero. Therefore, we decided to apply a two-step hurdle model to estimate the density for each two-month period. A first GAM to estimate the presence-absence as a Bernoulli distribution; and a second GAM to estimate the positive density as a lognormal distribution. The models were applied using R-INLA under the Bayesian statistics framework (Rue *et al.,* 2009, Lindgren *et al.,* 2011).

Covariates
Distance to coast, water depth, and fishing intensity (hours per month) were included in the model to predict herring gull density. To explore their relationships, a general additive model (GAM) was applied to each covariate to both the presence-absence as well as the positive density model (Figure 2-1 - Figure 2-3). It was known from previous studies that water depth exhibits a non-linear relationship with seabird densities (van Kooten *et al.,* 2019). Therefore, depth was modelled as a smoother using a cubic regression spline (knots=4, number of knots determined based on the expected shape of the effect to avoid overfitting and underfitting), while distance to coast and fishing intensity (log-transformed) were included as direct linear relationships. Additionally, birds could behave in clusters, due to some local habitat preference that are not captured by the 3 covariates. To capture such correlated spatial pattern, a spatial random effect (Gaussian Markov random field) was included in the model.
The main purpose of this study is to use environmental covariates to interpret and extrapolate density over the map, rather than understanding the causal relationships. Therefore, we did not apply strict rules to prevent confounding covariates, such as the relationship between depth and distance to coast.

Distance to coast effect to presence-absence

Distance to coast effect to positive density
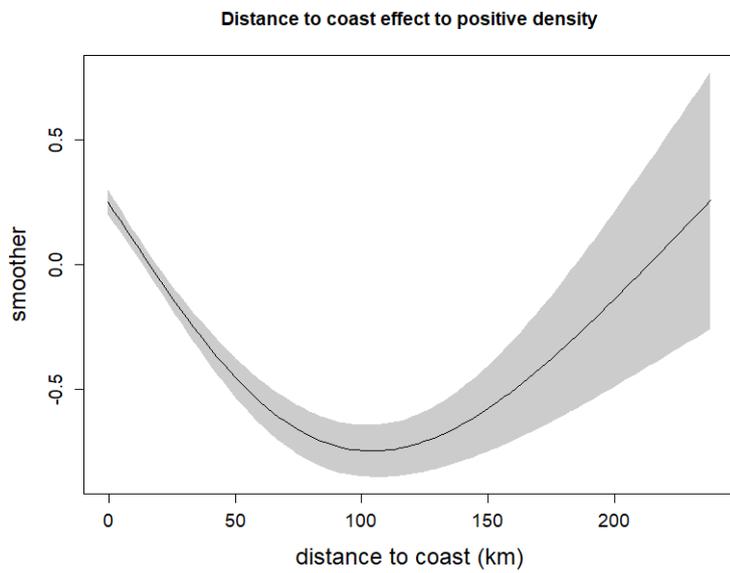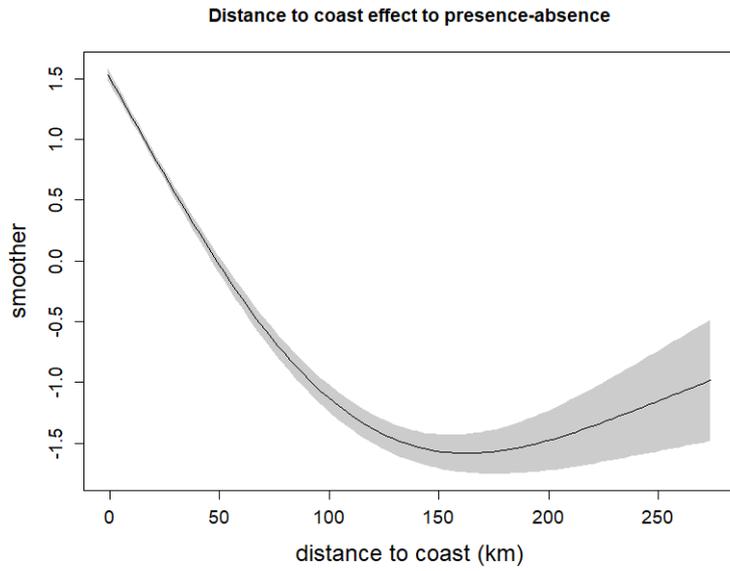
Figure 2-1 Estimated univariate effect of the distance to coast effect (smoother) in predicting presence-absence (top) and positive density (bottom) using a GAM.

Depth effect to presence-absence

Depth effect to positive density
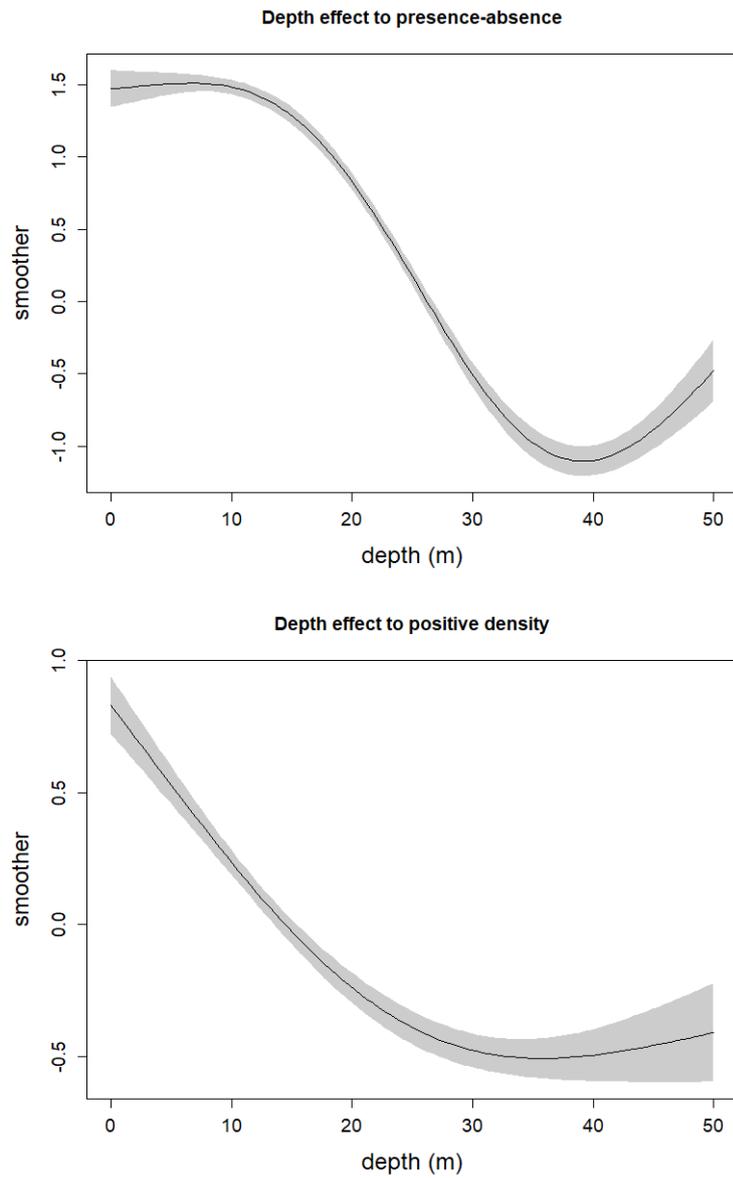
Figure 2-2 Estimated univariate water depth effect (smoother) in predicting presence-absence (top) and positive density (bottom) using a GAM.

Fishing effect to presence-absence

Fishing effect to positive density
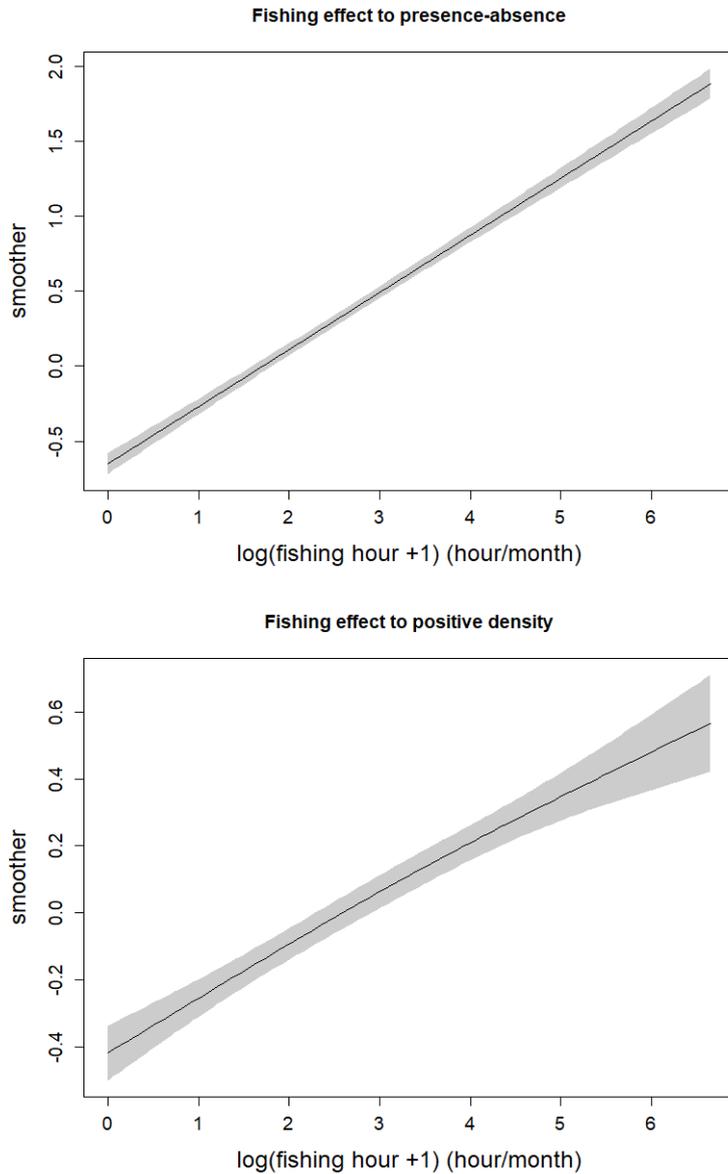
Figure 2-3 Estimated univariate, log-transformed fishing intensity effect (smoother) in predicting presence-absence (top) and positive density (bottom) using a GAM.

Detailed model description

The following Bernoulli GAM with time-invariant spatial random field was fitted for presence-absence of herring gulls:

$$bird_i^{01} \sim \text{Bernoulli}\,(\pi_i)$$

$$\text{E}\big(bird_i^{01}\big) = \pi_i\,, \qquad \text{var}\big(bird_i^{01}\big) = \pi_i \times (1 - \pi_i)$$

$$\text{logit}\big(bird_i^{01}\big) = intercept + f(depth) + dis\_coast_i + \log(fishing_{hour} + 1)_i + u_i$$

The response variable $bird_i^{01}$ refers to the absence and presence of the bird at location i, which follows a Bernoulli distribution with a probability π_i of presence. Model covariates include water depth ($depth$), distance to coast (dis_coast) and fishing intensity ($fishing_{hour}$). The water depth effect was modelled as a smoother using a cubic regression spline (knots = 4, number of knots determined based on the expected shape of the effect to avoid overfitting and underfitting), which is indicated by f. Additionally, a spatial random effect u_i was included to estimate the correlated spatial effect in bird densities. A model was applied for each two-monthly period independently.

The following log-normal GAM with time-invariant spatial random field was fitted for the positive density:

$$\log(bird_i^+) \sim \mathrm{N}\left(\omega_i, \sigma^2\right)$$

$$\mathrm{E}(\log(bird_i^+)) = \mu_i, \mathrm{var}(\log(bird_i^+)) = \sigma^2$$

$$\log(bird_i^+) = intercept + f(depth) + dis\_coast_i + dis\_\log(fishing_{hour} + 1)_i + u_i$$

The response variable $bird_i^+$ refers to the positive density of birds at location i. The log transformed density follows a Normal distribution (N) with mean ω_i and variance σ^2. To be consistent with the presence-absence model, the same covariates were kept in the log-normal GAM model. A model was applied for each two-monthly period independently.

The goal of the current exercise was to produce density predictions quickly. A model selection procedure was therefore not conducted. Such a procedure could potentially shed light on the predictive power of the model and its causal relationships.

The statistical analysis was conducted using R Core Team (2014) and the 'R-INLA' package (freely available at www.r-inla.org, Rue *et al.,* 2009, Lindgren *et al.,* 2011, Zuur *et al.,* 2017).
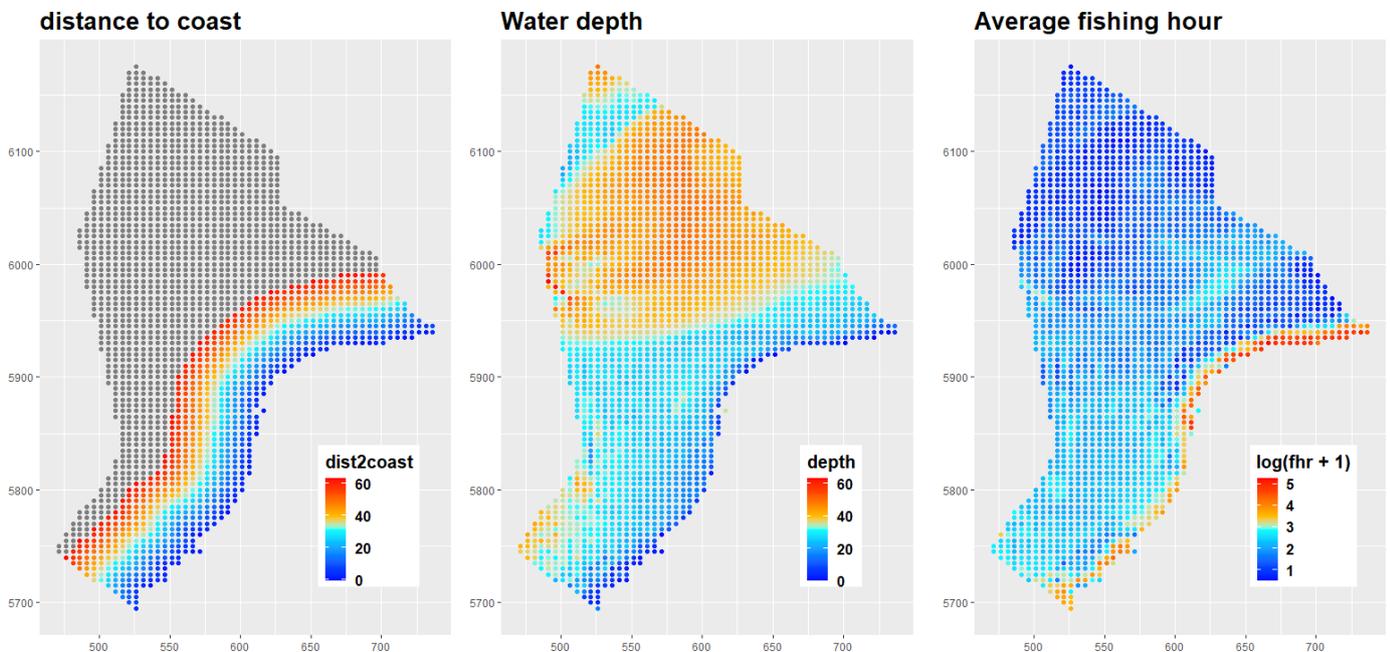
Figure 2-4 Map of distance to coast (km), water depth (m) and mean fishing intensity (hours/month; logged). These maps are used in predicting herring gull density.

Prediction maps

To obtain the distribution of the mean density map, we conducted a simulation-based approach. First, we simulated a set of regression parameters and spatial random effects from their joint posterior distribution, for both the presence-absence model (model 1) and positive model (model 2). From the parameters, we calculated the estimated presence probability as well as the positive density at each location of the map, given the depth, distance to coast and fishing intensity maps as shown in Figure 2-4. In model 2, since the response was based on log-transformed data, we applied the exponential function to back-transform its response to the original scale. The estimated mean density based on this set of parameters was then calculated by the multiplication of the response of model 1 and model 2 at each location on the map. In other words, the estimated densities are equal to the product of the probability that gulls occur in that grid cell times the density in that grid cell. We repeated this process a 1000 times. As a result, a marginal posterior distribution for the mean density was obtained from the 1000 simulations at each location of the map. From those simulations, the median was used as the

value for the mean map, and the 2.5% and 97.5% percentiles were used as the 95% credible intervals (the Bayesian analogue to confidence intervals).

2.5   Collision risk and population level effects of collisions

To predict the number of casualties due to collisions with OWFs, the bird densities in OWF areas were determined, converted to fluxes and used in the BAND model to predict the number of casualties per OWF search area as described by Potiek *et al.* in the main KEC 4.0 report (2022). Also, the population models used to predict the population-level effects of the casualties, 'Acceptable Level of Impact' thresholds against which the population-level effects were tested and scenarios used, were identical to those used in the main KEC 4.0 report (Potiek *et al.* 2022). Collision mortality probabilities were calculated based on the newly estimated number of casualties and updated total number of individuals present on the Dutch Continental Shelf following the method described by Potiek *et al.* in the main KEC 4.0 report (2022).

3 Results

3.1 Old maps inverse distance weighting with spreading

The figures of the maps in the main report show clearly that the extreme high values in the data are spread out over a square area around these high values (Figure 3-1, Figure 3-2). A clear example is the area close to the west coast of the Netherlands in the map of April-May (Figure 3-1). Another striking result of the used method is that the flight route that is used during counts can sometimes been seen in the maps. The areas that are visited by the airplane, often show a lower density of gulls than their surroundings. This might be an artifact of the high number of zeros in the data. An example is the north part of the NCP in the map of October-November (Figure 3-1). We also included a map in which we only selected data between 2010-2018 (Figure 3-2). In this way, we can compare methods for which only a shorter timeframe has been used in the analysis. However, both maps look fairly similar.

IDW - original data, high densities spread with square
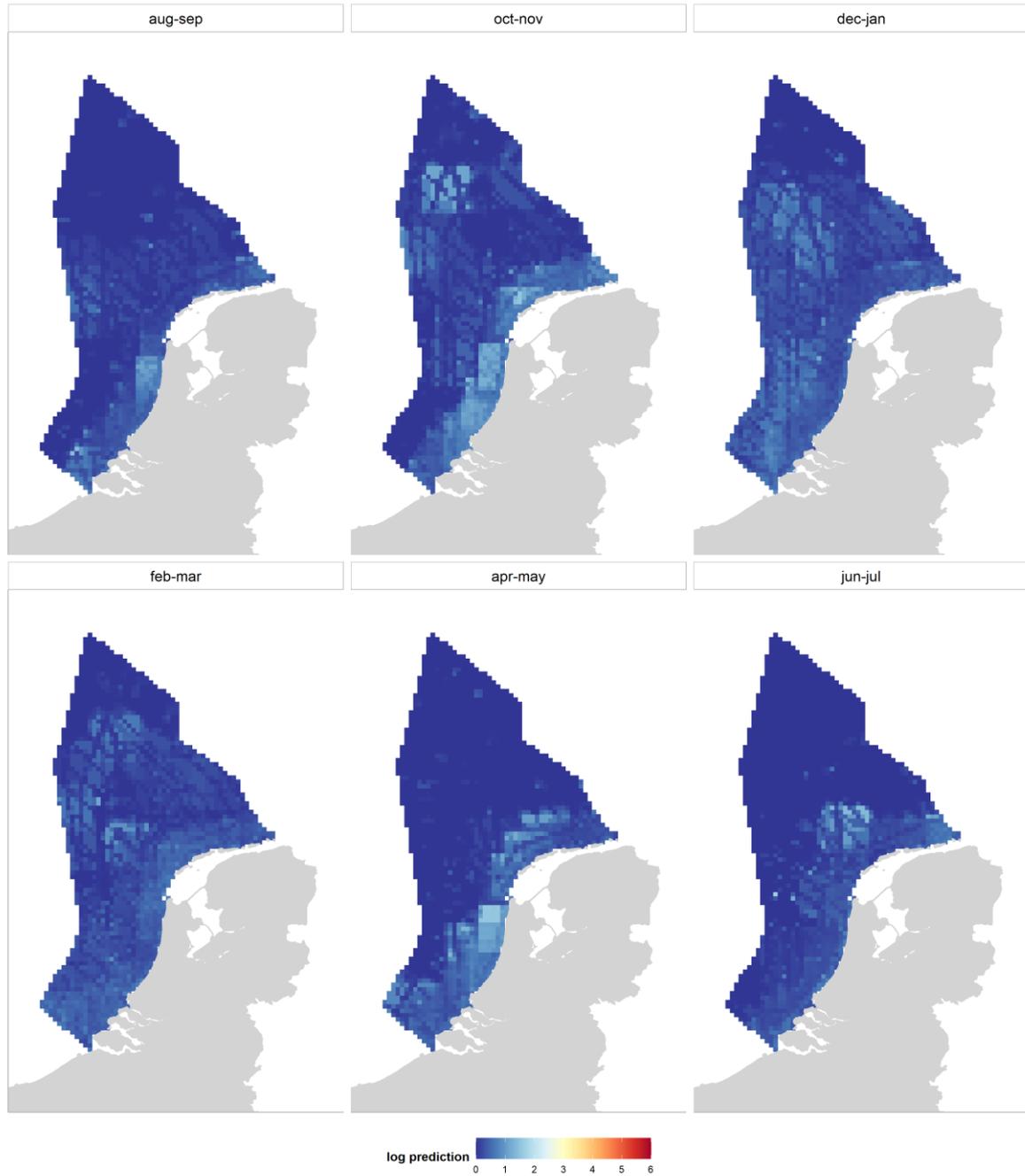
Figure 3-1 IDW density map (individuals/km^2) based on the original method, data between 2000-2020 (spreading the values using squares, log scale).

IDW - 2010-2018 data, high densities spread with square
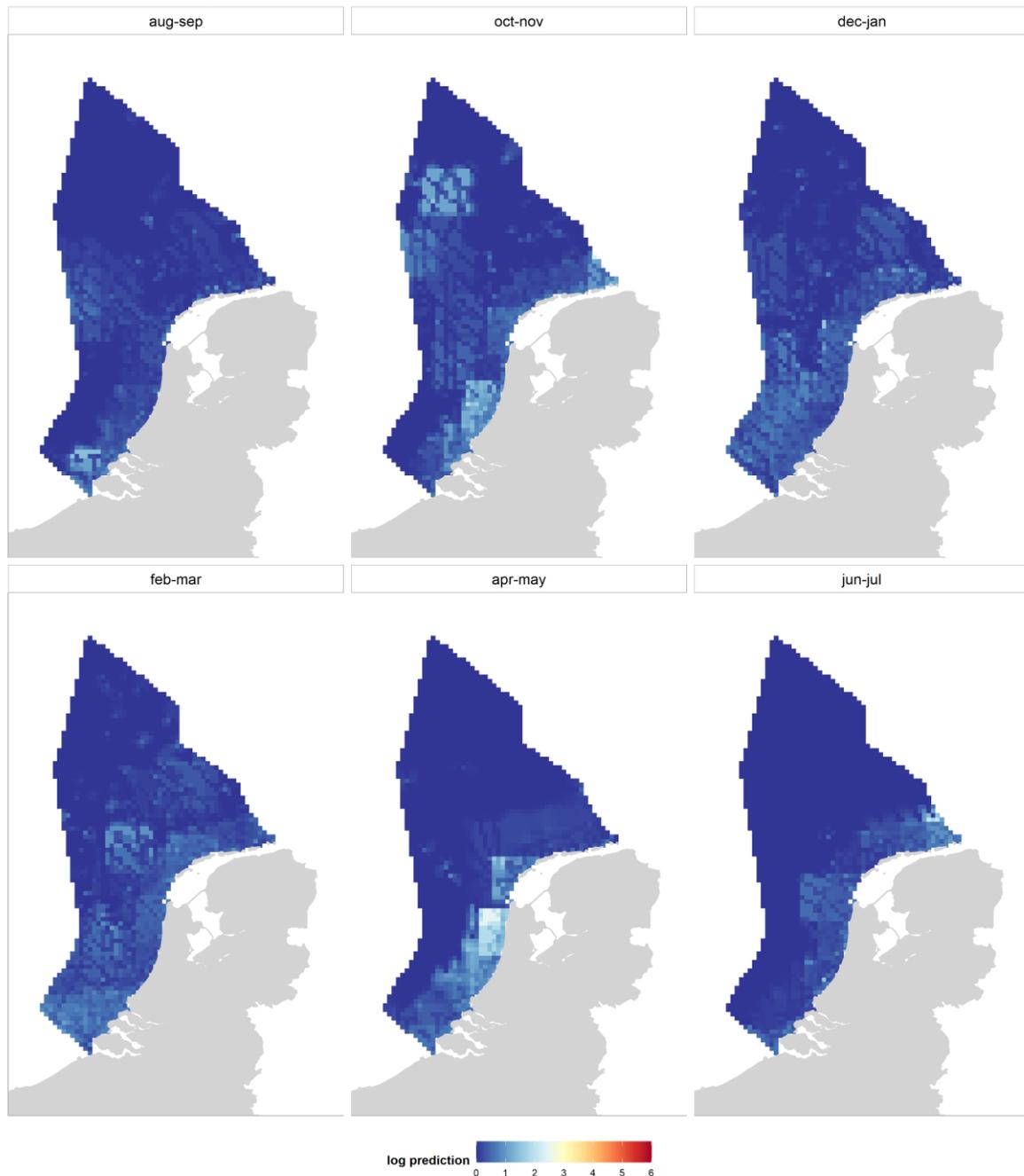
Figure 3-2 IDW density map (individuals/km^2) based on the original method, data between 2010-2018 (spreading the values using squares, log scale).

3.2   Inverse distance weighting

The map in which inverse distance weighting was performed on data without spreading of the data shows a map which is highly scattered. The hotspots are clearly seen as single high values in the map (Figure 3-3). Spreading the high density observations with a kernel before performing the inverse distance weighting results in maps that look fairly similar to the maps based on the original method (Figure 3-4). Furthermore, spreading data over an area around observations with high densities close to the coast results in losing a certain amount of gull observations when the kernel spreading projects observations on land. Additionally, the flight route patterns can still be seen in the maps, just as in the maps of the previous method, for instance in the map of October-November (Figure 3-4).
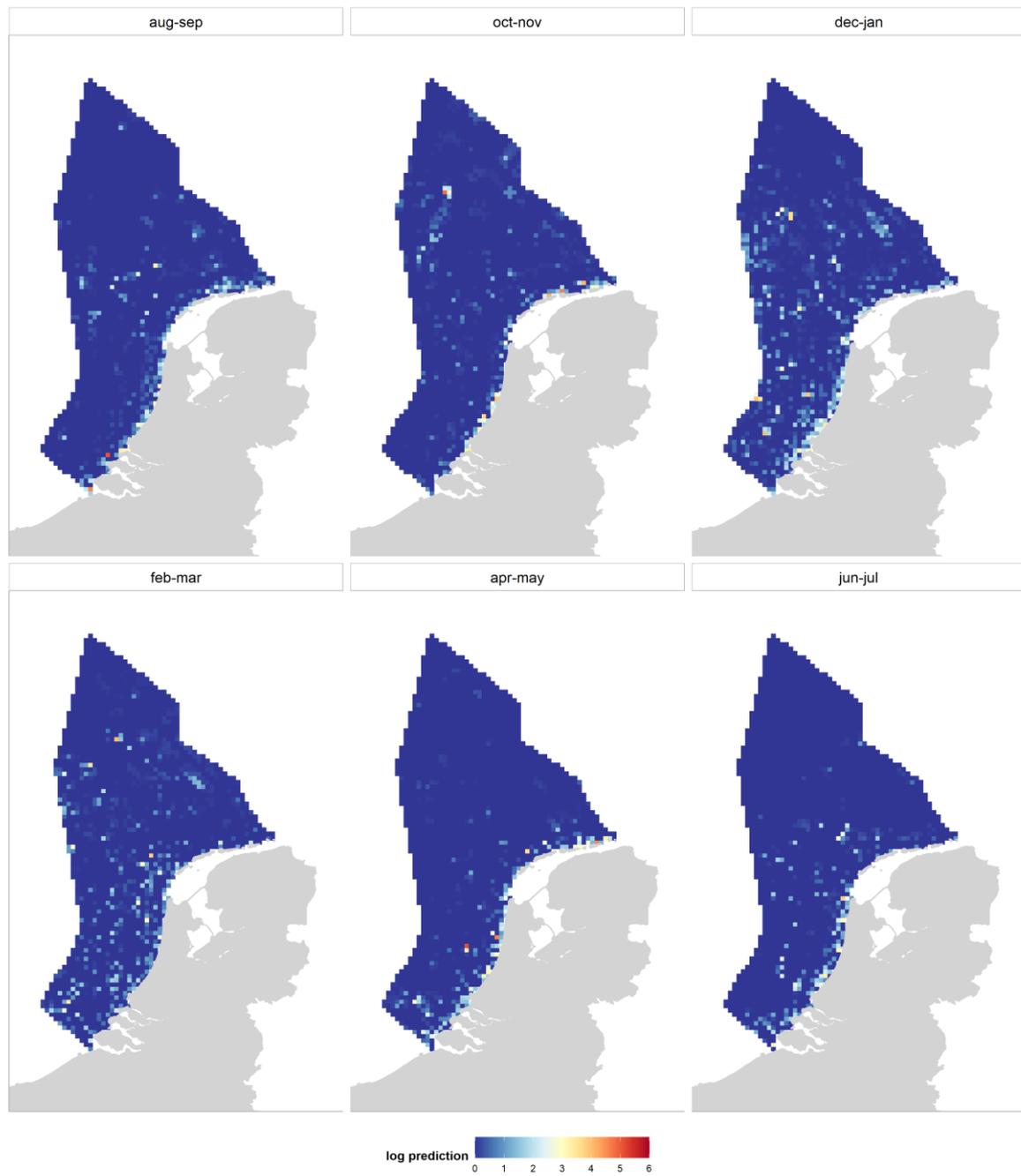
Figure 3-3 IDW density map (individuals/km^2) based on the raw data, data between 2000-2020 (log scale).

IDW - high densities spread with gaussian kernel
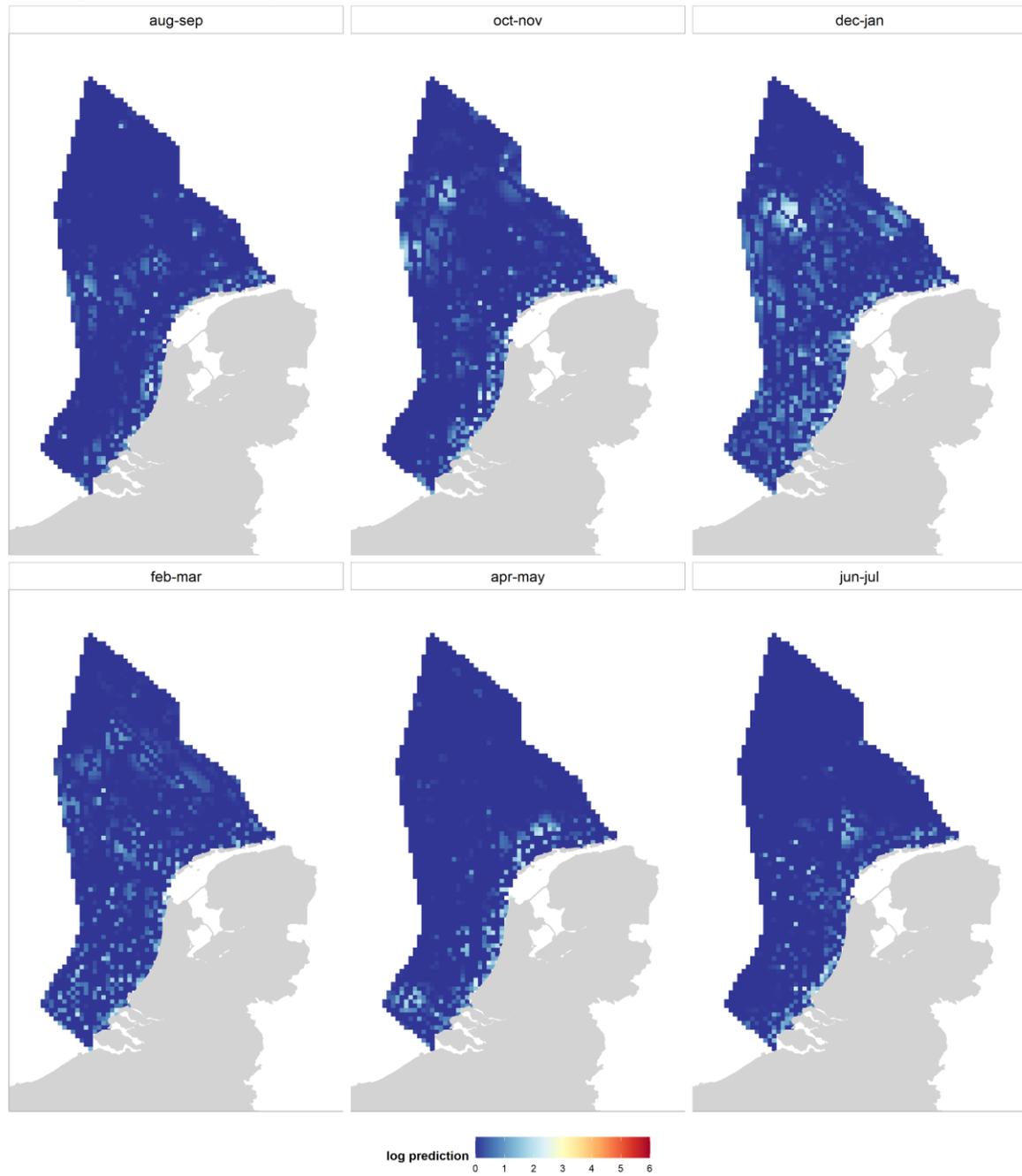
Figure 3-4 IDW density map (individuals/km^2) based on data with high densities spread out with kernels, data between 2000-2020 (log scale).

3.3   Kriging

The map in which kriging was performed with covariate distance to coast shows that the density of gulls is almost zero further at sea (Figure 3-5). This result can be clearly seen in all periods except for the period August-September. Otherwise, the maps of the consecutive periods differ greatly. Especially maps for April-May and August-September stand out. Again the map of April-May shows the flight route patterns, as has been observed in the previous maps. In addition to kriging with distance to coast, kriging was also performed with the covariates distance to coast and fishing activity. These latter maps look very similar to the maps based on kriging with distance to coast only and have therefore not been included in this memo. It should be noted that kriging predicts densities below zero at places where very low amount of numbers are expected. This is for instance the case for the period April-May far offshore.

kriging with covariate distance to coast
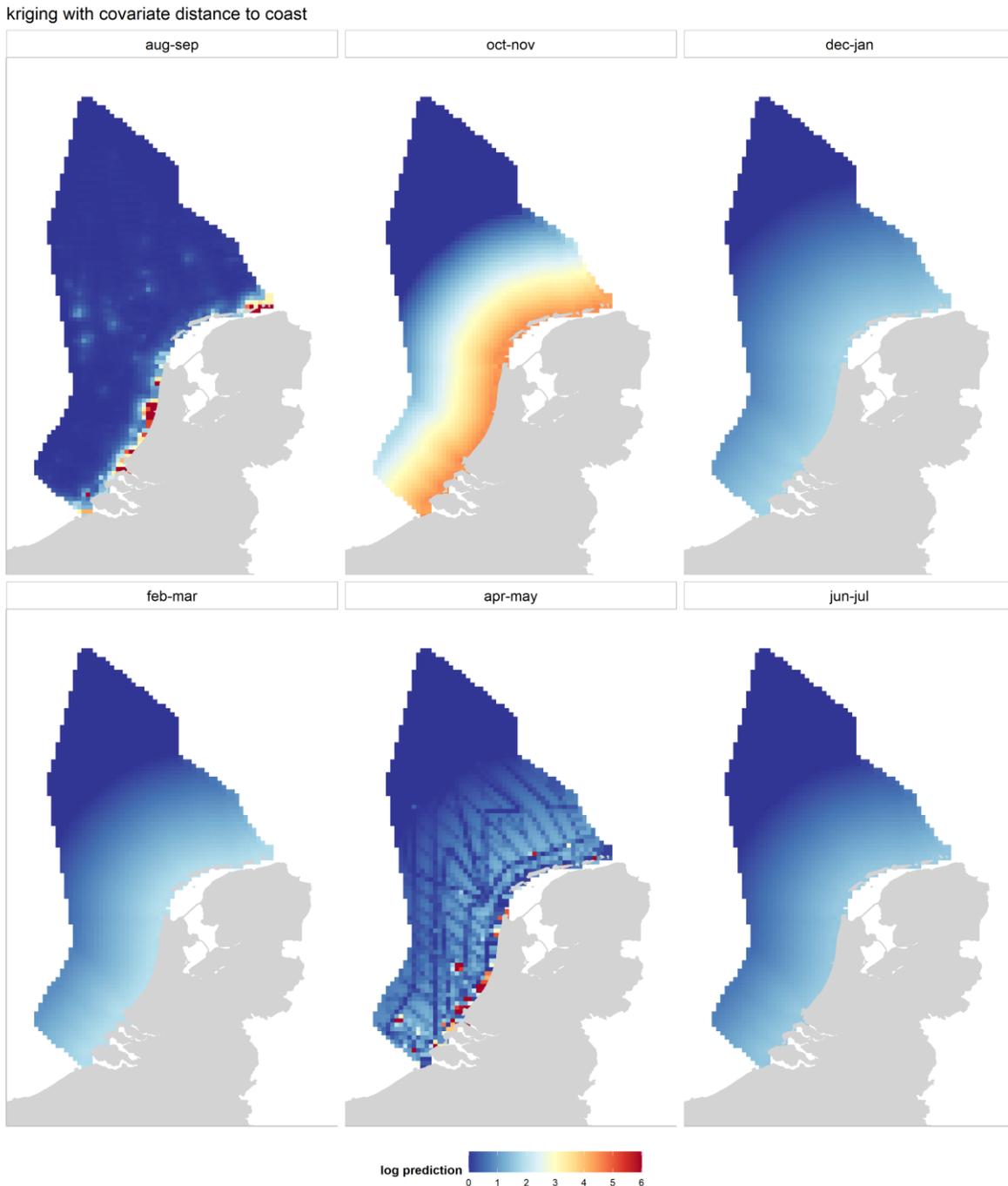
Figure 3-5 Kriging density map (individuals/km²) with covariate distance to coast of all data (2000-2020). Predictions below zero are set to zero, and predictions > 6 were set to 6 in this map (log scale).

3.4   INLA regression model

The maps of the mean predictions from the regression (INLA) model show clearly that highest densities of herring gulls are expected in the coastal area (Figure 3-6). Densities further at sea are expected to be very low. This is consistent with the major effects from water depth and distance to coast in the model. An exception is an area close to the British part of the sea in the North-West of the NCP. Here, a 'line' with relatively higher expected densities can be seen in for instance the map of October-November. This line matches a pattern in the covariates (Figure 2-4) of relatively high fishing intensity and deep water. Flight route patterns are not visible in the map, which is the case in some of the maps based on the other methods. In addition to the mean density map, the lower and higher bound maps illustrate the uncertainty of the mean density at the given location (Figure 3-7). From these maps, it can for example be observed that the 'line' in the map described above, with relatively higher expected densities, is an area with a relatively high uncertainty. In addition, densities closer to the coast are more uncertain. This is an indication that there is high variability in the observations in these areas.

Regression model prediction maps, data 2010-2018
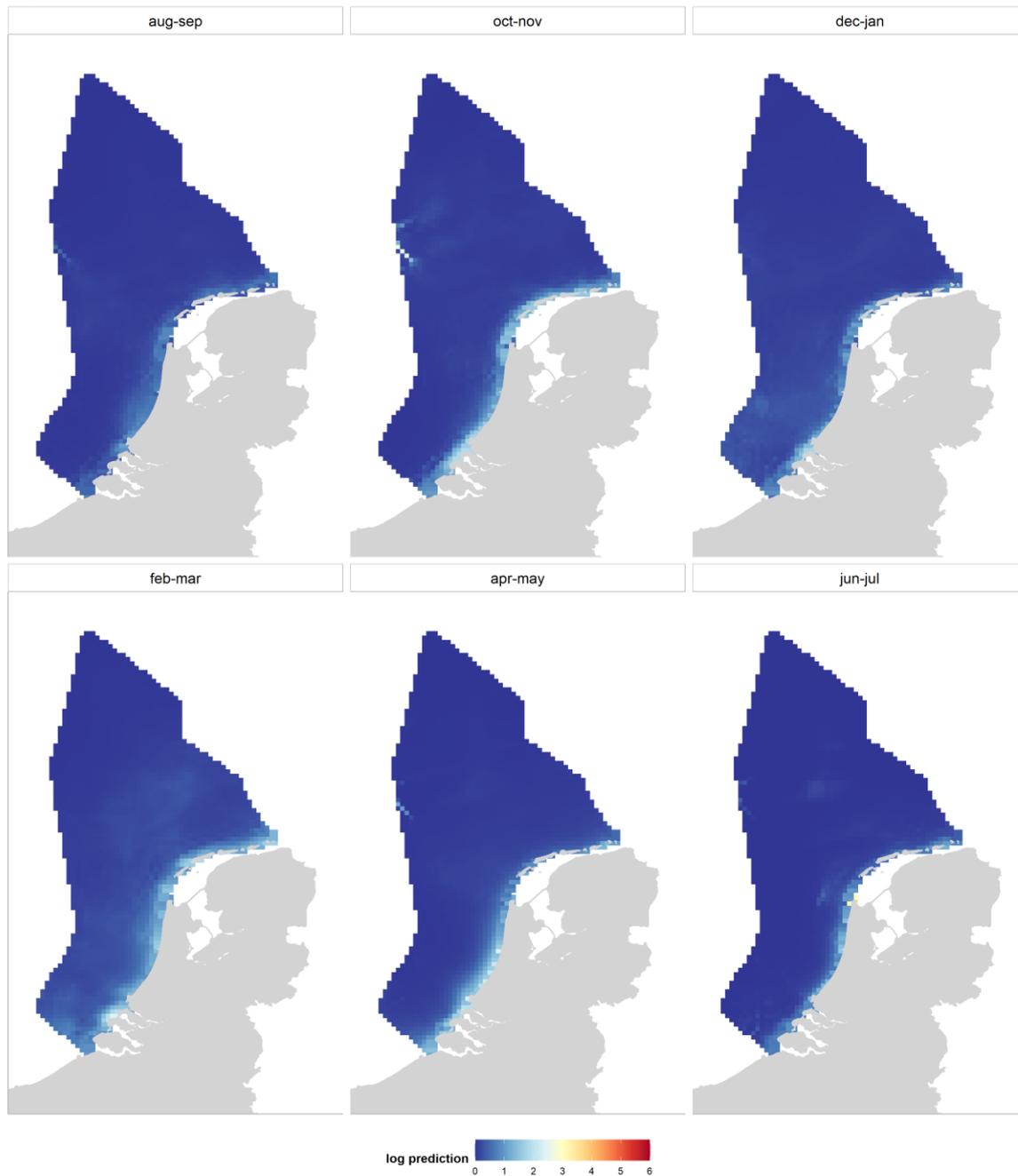
Figure 3-6 Regression model predicted density map (individuals/km^2) with the mean of predictions from the model with data between 2010-2018 (log scale). The regression model includes the covariates distance to coast, depth and fishing effort.
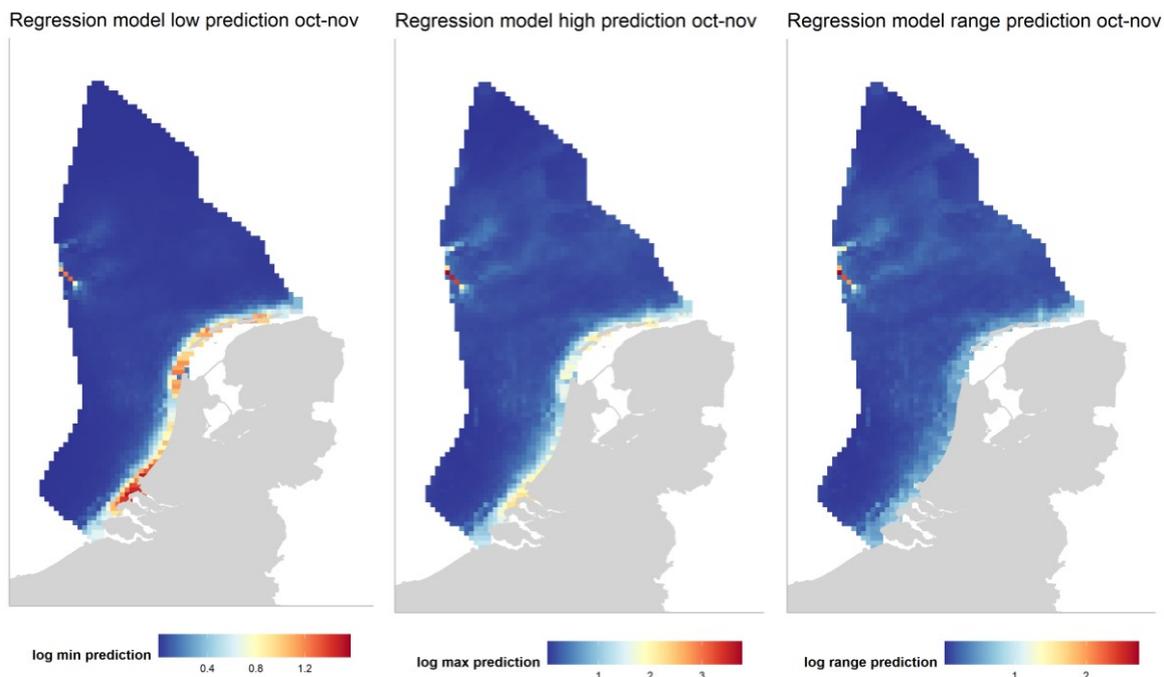
Figure 3-7 Lower bound, higher bound and range (95% credible intervals) of the density (individuals/km^2) values predicted by the INLA regression model for the period October–November (log scale). Note that the scale differs between panels to allow for maximal contrast between the values.

3.5   Comparison total densities per time period

The total densities per density map give an indication of the total number of herring gulls occupying the Dutch Continental Shelve per period. The maps based on the raw data show higher total densities than the original maps, especially in December-January and April-May. The maps based on the data with spreading of high densities with Gaussian kernels show lower densities than the original maps, except for December-January. Especially the estimate for October-November is much lower. The maps based on kriging show the highest total densities of all maps. Compared to the original maps, the estimates are about 5-fold higher. The maps based on the regression model show lower total densities than the original maps based on data in the same period (2010-2018), except for February-March. All estimates are in the same order of magnitude, except for the maps based on kriging.

Table 1 Total density estimates based on the different density maps. The density maps were based on the original method (original), raw data without spreading the high densities (raw data), data with spreading high densities with gaussian kernels (Gaussian), kriging with the covariate distance to coast (Kriging), the original data with only observations between 2010-2018 (Original (2010-2018)), or the regression model with only observations between 2010-2018 (Regression (2010-2018)).

Period	Original	Raw data	Gaussian	Kriging	Original (2010-2018)	Regression (2010-2018)
Aug-Sep	8851	19509	7789	11703	7064	6227
Oct-Nov	21771	23702	13481	106227	18805	14014
Dec-Jan	18526	30128	21466	48947	12247	10452
Feb-Mar	15269	17865	12426	48461	13831	19487
Apr-May	14297	25241	10515	28880	19398	12417
Jun-Jul	8953	12453	7970	37964	6659	5602

3.6 Collision victims

The INLA regression density maps result in new bird densities inside wind farms, and hence a change in predicted causalities due to collisions. The predicted annual numbers of collision victims are clearly lower compared to previously used density map (Table 2). The estimated number of collision casualties based on the previous density maps was 236, while the new density maps result in 138 casualties. The most profound change is seen for Hollandse Kust Noord, with an estimate of 8 casualties compared to 26 casualties based on the previous density maps. The highest numbers of casualties are estimated for the different subareas within Hollandse Kust Zuid. The estimated casualties are highest for the period February-March (Table 3), and lowest in June-July.

Table 2 Number of predicted collision victims per wind farm based on the updated national density maps, in comparison to the original density maps.

	Annual number of collisions		
Wind farm	**INLA density map**	**Original density map**	**Difference**
Borssele 2	5.1	7.3	- 2.2
Borssele 3	3.5	4.8	- 1.3
Borssele 4 - Blauwwind	2.6	3.8	- 1.2
Borssele Site V -Two towers	0.2	0.3	- 0.1
Egmond aan Zee	8.5	10.2	- 1.7
Prinses Amaliawindpark	6.1	16	- 9.9
Eneco Luchterduinen	4.9	8.4	- 3.5
Gemini Zee energie	1.7	1.6	+ 0.1
Gemini Buitengaats	1.6	1.9	- 0.3
Hollandse Kust Zuid Holland IV	12.9	17.5	- 4.6
Hollandse Kust Zuid Holland III	12.4	17.3	- 4.9
Hollandse Kust Zuid Holland II	7.4	15.2	- 7.8
Hollandse Kust Zuid Holland I	7.5	14.8	- 7.3
Borssele 1	4.1	5.9	- 1.8
Hollandse Kust Noord (Tender 2019)	8.4	26.1	- 17.7
Ten noorden van de Waddeneilanden	1.6	1.5	+ 0.1
IJmuiden Ver	8.7	16.1	- 7.4
Hollandse Kust West	4.4	11.1	- 6.7
Hollandse Kust West zuidelijke punt	1.8	4.6	- 2.8
Zoekgebied 1 Noord	6.7	12.3	- 5.6
Zoekgebied 5 Oost origineel	9.2	11.3	- 2.1
IJmuiden Ver Noord	5.1	7.6	- 2.5
Zoekgebied 1 Zuid	3	4.4	- 1.4
Zoekgebied 2 Noord	10.6	15.5	- 4.9
SUM	**138**	**236**	**- 98**

Table 3 Number of predicted collision victims period, based on the updated national density maps.

Wind farm	**Aug-Sept**	**Oct-Nov**	**Dec-Jan**	**Feb-Mar**	**Apr-May**	**Jun-Jul**
Borssele 2	0.28	0.22	0.54	2.42	1.26	0.42
Borssele 3	0.16	0.11	0.48	1.79	0.70	0.24
Borssele 4 - Blauwwind	0.10	0.05	0.51	1.38	0.46	0.15
Borssele Site V -Two towers	0.01	0.00	0.02	0.09	0.03	0.01
Egmond aan Zee	0.95	0.84	0.65	2.32	2.26	1.52
Prinses Amaliawindpark	0.97	0.60	0.75	2.10	1.25	0.41

Eneco Luchterduinen	1.20	0.60	0.58	1.10	1.17	0.22
Gemini Zee energie	0.29	0.22	0.24	0.53	0.34	0.08
Gemini Buitengaats	0.27	0.19	0.21	0.51	0.37	0.07
Hollandse Kust Zuid Holland IV	2.81	1.62	1.23	2.49	3.97	0.76
Hollandse Kust Zuid Holland III	2.47	1.43	1.28	2.30	4.26	0.65
Hollandse Kust Zuid Holland II	1.70	0.80	1.16	1.58	1.90	0.26
Hollandse Kust Zuid Holland I	1.76	0.86	1.15	1.74	1.67	0.27
Borssele 1	0.17	0.11	0.57	2.00	0.81	0.39
Hollandse Kust Noord (Tender 2019)	1.17	0.88	0.95	3.02	1.69	0.63
Ten noorden van de Waddeneilanden	0.26	0.22	0.24	0.53	0.27	0.08
IJmuiden Ver	1.02	1.05	2.13	3.89	0.59	0.02
Hollandse Kust West	0.35	0.55	1.14	1.96	0.33	0.04
Hollandse Kust West zuidelijke punt	0.11	0.14	0.60	0.81	0.11	0.01
Zoekgebied 1 Noord	2.01	0.93	1.30	1.50	0.92	0.00
Zoekgebied 5 Oost origineel	1.29	1.55	1.35	3.80	1.10	0.08
IJmuiden Ver Noord	0.84	0.78	1.03	1.70	0.75	0.03
Zoekgebied 1 Zuid	0.81	0.31	0.65	0.99	0.23	0.00
Zoekgebied 2 Noord	1.95	1.30	1.44	2.73	2.64	0.49
SUM	**23**	**15**	**20**	**43**	**29**	**7**

3.7   Population-level impact

The new density maps resulted in the survival rates as reported in Table 4. The effects of these adjusted survival rates on the population-level are shown in Table 4. The median population growth rate (lambda) changed as a result of the impact from 0.952 to 0.945-0.947, depending on the scenario. In Table 5, Pcasualty gives the probability that the violation of the threshold population size (X, for this species a 15% decline over 30 years or 3 generations compared to the null scenario) is caused by the impact and not by uncertainty in the population models. For this species, the probability that a population abundance is 15% lower than the null scenario as result of the impact is between 13% and 16.5%, depending on the scenario. This exceeds the acceptable probability of 10% of such a decline, meaning that the ALI is violated for each of the scenarios.

Table 4 OWF mortality for each scenario (mean casualties per two-month period / max abundance), and stage-specific survival rates (S_0, juvenile survival age 0; S_J, immature survival age 2-4, S_A, adult survival age >4) including OWF mortality.

Scenario	Mean casualties per two-month period	Max abundance	OWF mortality	survival S_0	survival S_J	survival S_A
Null	0	19,487	0.000	0.375	0.800	0.865
Basic_2030	17	19,487	0.005	0.372	0.798	0.860
Rekenvariant_I	22	19,487	0.007	0.371	0.797	0.859
Rekenvariant_II	22	19,487	0.007	0.371	0.797	0.859
Rekenvariant_III	23	19,487	0.007	0.370	0.797	0.858

Table 5 Summary herring gull population level effects; the median, 5% and 95% percentiles of the population growth rates (lambda) are reported. X represents the decrease in population abundance that is maximally allowed compared to the situation without OWFs. $P_{casualty}$ represents the probability that a violation of the X threshold results from an OWF induced impact. ALI represents the 'Acceptable Level of Impact' and the last column shows whether $P_{casualty}$ violates the ALI threshold.

	Lambda			$P_{casualty}$	
Scenario	Median	5th percentile	95th percentile	(X = 15%)	ALI 0.1

Null	0.952	0.893	0.999	NA	NA
Basic_2030	0.947	0.887	0.993	0.131	TRUE
Rekenvariant_I	0.946	0.886	0.992	0.154	TRUE
Rekenvariant_II	0.945	0.886	0.992	0.157	TRUE
Rekenvariant_III	0.945	0.886	0.992	0.165	TRUE

4   Conclusions and recommendations

In this memo, additional exploratory analyses of herring gull density maps are described. The density maps of some of the seabirds species under assessment in KEC 4.0 showed some unexpected spatial patterns. The herring gull is a coastally oriented species, while the original maps predicted relatively high densities of herring gulls further away from the coast. The high densities further offshore are likely to be the result of herring gulls that gather behind fishing vessels. Therefore additional analyses were conducted in order to arrive at maps that represent the observed patterns better. Five different methods were used to produce density maps of herring gulls. The results of the exploratory analyses described here, suggest that density maps based on a spatial, INLA regression model give a more representable spatial pattern of the herring gull than the methods previously used and alternatives investigated in this study. The quality and spread of the available bird observational data are discussed in the main KEC 4.0 report (Soudijn *et al.* 2022). Below, we discuss the results of all the methods that were explored. Further analyses are needed to resolve the covariates that best describe density distributions of herring gulls.

For the original density maps, inverse distance weighting (IDW) was performed on data for which high density observations were spread out in squared areas of 55x55 km. Here, results of two methods of inverse distance weighting (IDW) are described; 1. IDW of observational data with no spreading of the high density observations and 2. IDW of data for which high density observations were spread out using kernels. Both methods resulted in maps that were not an improvement compared to the original maps. Using the first method, herring gull density maps showed highly scattered densities because of the high spatial-temporal variability of the high density observations. Using the second method, herring gull density maps look very comparable to the original maps in which high densities were spread out using squares. The maps show distributions that are not considered realistic, with high herring gull densities far offshore where they are normally not expected due to their coastal orientation. It is possible that these high densities are the results of a few high density observations of herring gulls gathered behind a fishing vessel, or of the spreading of the high density observations, pushing the observations far offshore. In addition, the survey airplane flying routes are visible in the maps as relatively low densities. This is probably a result of high amounts of zero observations along the survey route. Besides, spreading the data around a spatial position (either with squares or kernels) projects some of the observed birds from the sea up to the land. These birds are hereby lost from the density maps, as our analysis only covers the sea area. In conclusion, spreading high density observations seems odd, given that these are "real" observations and spreading leads to strange artefactual patterns in the density maps, in the form of recognizable squares or kernels. IDW seems to handle zero-inflated data and high spatiotemporal variability in high density observations poorly.

Two additional sets of density maps were created using kriging; kriging of the observations was done using 1. The covariate distance to coast and 2. The covariates distance to coast and fishing activity (results not shown). Both sets of maps based on kriging predict high densities close to the coast and densities of almost zero further offshore. Yet, kriging does not seem a very suitable technique for our purpose, as kriging predicts densities below zero at locations where very low numbers are expected. Besides, the maps of the different periods look extremely different from each other. This is not expected based on herring gull behaviour, except for differences in distribution between the winter and breeding period. Similar to the IDW maps, survey airplane flying routes are visible as relatively low densities in one of the maps. In conclusion, kriging does not seem a suitable technique for our purpose. Like IDW, kriging seems to handle zero-inflated data and high spatiotemporal variability in high density observations poorly.

The set of density maps that are based on the spatial regression model with covariates distance to coast, fishing activity and water depth, shows herring gull distributions with high densities along the Dutch coast. This pattern is expected as the herring gull is a coastally oriented bird and is only seen occasionally further away from the coast (van Donk *et al.* 2019, Vanermen *et al.* 2020). Some higher

densities are observed further away from the coast, which are probably due to fishing activity in that area. Flight route patterns are not visible in the maps. The two step spatial regression model that we designed can handle zero-inflated data and high spatiotemporal variability in high density observations. Since we had little time available for our analysis, it should be stressed that the results described here are only preliminary. Yet, the maps predicted by our regression model are similar to the maps presented by Waggitt *et al.* (2020). Waggitt *et al.* (2020) mapped herring gull densities for two six-month periods and covered the full North Sea. An interesting prediction in our maps, which is also shown by Waggit et al. (2020), is an area with relatively high densities close to the British part of the sea in the North-West of the NCP. Here, a 'line' with relatively higher expected densities can be seen in a couple of periods. This is probably caused by a combination of high fishing intensity by British fishing vessels on *nephrops* and a relatively deep part of the sea.

Further work should include a model selection procedure to determine the covariates that best describe the herring gull density for each of the two-month periods. The factors that influence herring gull density are definitely not limited to the 3 covariates included in the model. For instance, no information of colony location was included in the model. This is an important covariate during the breeding season (April-August). The spatial random effects in the model are expected to capture some of the unknown spatial effects. However, more detailed spatial information on factors that affect herring gulls are expected to improve the accuracy of the regression model. The covariate for fishing activity was only available for a period between 2010-2018 and on a monthly basis and we were therefore not able to include all bird observational data. Moreover, it is questionable if the accumulated number of fishing hours per month give a good representation of the fishing activity that the herring gull are interested in. A more elaborate analysis of fishing activity data, such as VMS data, may give a more reliable estimate of fishing activity. In addition, the performance of the model should be tested by comparing the model predictions to the original data, for example, posterior predictive checks could be conducted on the observed data using simulations. An interesting question is, how well the model actually predicts the high densities of herring gulls that are observed in the data. As for all statistical models, density estimations outside sampled areas are interpolated purely based on assumptions and mathematical tools, and should thus be interpreted with caution.

A clear advantage of the regression model approach is the possibility to include confidence intervals around the estimated values. These indicate the level of variability of the estimations and the reliability of density estimations in a certain area. The confidence intervals could be used to calculate confidence intervals around the casualty estimations and collision mortalities and could hereby contribute to the communication of uncertainty in the outcomes of the KEC assessments.

The estimated causalities are highest for the two-month period February-March and lowest in June-July. The latter matches the period when most individuals are breeding, partly outside the Netherlands. Compared to the main KEC 4.0 results, lower numbers of casualties were estimated with the density maps based on the regression model. The ALIs were still exceeded for all scenarios. This can be partly due to the fact that also the maximum abundance was estimated to be lower by the density maps based on the regression model (19,487 vs. 21,139 originally). Still, the OWF mortality probability values were found to be slightly lower based on the regression model for all scenarios (0.005-0.007) than for the original density maps (0.008-0.011).

In conclusion, our exploratory analysis shows that the density maps that are created based on the regression models look the most promising. Additional research is needed to complete the model and make it fully suitable to be used in an assessment framework such as KEC. The current analysis focused on possible methods to improve the density maps of the herring gull, other uncertainties or knowledge gaps for the herring gull were not considered here. We refer to the main report of KEC 4.0 for a full discussion of data availability in national and international waters and other shortcomings in the assessment framework (Potiek et al. 2022, Soudijn et al. 2022).

5 Quality Assurance

Wageningen Marine Research utilises an ISO 9001:2015 certified quality management system. The organisation has been certified since 27 February 2001. The certification was issued by DNV.

References

van Donk, S., J. Shamoun-Baranes, J. van der Meer, and K. C. J. Camphuysen. 2019. Foraging for high caloric anthropogenic prey is energetically costly. Movement Ecology 7:17.

van Kooten, T., F. Soudijn, I. Tulp, C. Chen, D. Benden, and M. Leopold. 2019. The consequences of seabird habitat loss from offshore wind turbines, version 2 : Displacement and population level effects in 5 selected species. Wageningen Marine Research, IJmuiden.

Leopold, M. F., M. Boonman, M. P. Collier, N. Davaasuren, R. C. Fijn, A. Gyimesi, J. de Jong, R. H. Jongbloed, B. Jonge Poerink, J. C. Kleyheeg-Hartman, K. L. Krijgsveld, S. Lagerveld, R. Lensink, M. J. M. Poot, van der W. J.T, and M. Scholl. 2014. A first approach to deal with cumulative effects on birds and bats of offshore wind farms and other human activities in the Southern North Sea. IMARES Report C166/14, IMARES.

Lindgren, F., H. Rue, and J. Lindström. 2011. An explicit link between Gaussian fields and Gaussian Markov random fields: the stochastic partial differential equation approach. Journal of the Royal Statistical Society: Series B (Statistical Methodology) 73:423–498.

Potiek, A., J. J. Leemans, R. P. Middelveld, and A. Gyimesi. 2022. Cumulative impact assessment of collisions with existing and planned offshore wind turbines in the southern North Sea. Analysis of additional mortality using collision rate modelling and impact assessment based on population modelling for the KEC 4.0. Bureau Waardenburg Report, 21-205, Bureau Waardenburg, Culemborg.

R Core Team. 2014. R: A language and environment for statistical computing. Page R Foundation for Statistical Computing. www.r-project.org, Vienna, Austria.

Rue, H., S. Martino, and N. Chopin. 2009. Approximate Bayesian inference for latent Gaussian models by using integrated nested Laplace approximations. Journal of the Royal Statistical Society: Series B (Statistical Methodology) 71:319–392.

Soudijn, F. H., S. van Donk, M. F. Leopold, J. T. van der Wal, and V. Hin. 2022. Cumulative population-level effects of habitat loss on seabirds 'Kader Ecologie en Cumulatie 4.0.' Wageningen Marine research report C007/22, Wageningen Marine Research, IJmuiden.

Vanermen, N., S. Lilipaly, H. Verstraete, and R. C. Fijn. 2020. Tracking lesser black-backed and herring gulls in the Dutch Delta and data on breeding success and foraging ecology. Progress Report 2020, Bureau Waardenburg Report 20-279, Bureau Waardenburg, Culemborg.

Waggitt, J. J., P. G. H. Evans, J. Andrade, A. N. Banks, O. Boisseau, M. Bolton, G. Bradbury, T. Brereton, C. J. Camphuysen, J. Durinck, T. Felce, R. C. Fijn, I. Garcia-Baron, S. Garthe, S. C. V. Geelhoed, A. Gilles, M. Goodall, J. Haelters, S. Hamilton, L. Hartny-Mills, N. Hodgins, K. James, M. Jessopp, A. S. Kavanagh, M. Leopold, K. Lohrengel, M. Louzao, N. Markones, J. Martínez-Cedeira, O. Ó Cadhla, S. L. Perry, G. J. Pierce, V. Ridoux, K. P. Robinson, M. B. Santos, C. Saavedra, H. Skov, E. W. M. Stienen, S. Sveegaard, P. Thompson, N. Vanermen, D. Wall, A. Webb, J. Wilson, S. Wanless, and J. G. Hiddink. 2020. Distribution maps of cetacean and seabird populations in the North-East Atlantic. Journal of Applied Ecology 57:253–269.

van der Wal, J. T., M. E. B. van Puijenbroek, and M. F. Leopold. 2018. Cumulatieve effecten van offshore wind parken: habitatverlies zeevogels: update voor vijf zeevogelsoorten tot 2030. Wageningen Marine Research rapport C059/18, Wageningen Marine Research.

Zuur, A. F., E. N. Ieno, A. A. Savel'ev, and A. F. Zuur. 2017. Beginner's guide to spatial, temporal and spatial-temporal ecological data analysis with R-INLA. Highland Statistics Ltd, Newburgh, United Kingdom.

Justification

Report C010/22
Project Number: 4315100166

The scientific quality of this report has been peer reviewed by a colleague scientist and a member of the Management Team of Wageningen Marine Research

Approved: Dr. I.Y.M. Tulp
                 Researcher

Signature:

Date: 7th of March 2022

Approved: Drs. J. Asjes
                 Manager Integration

Signature:

Date: 7th of March 2022

With knowledge, independent scientific research and advice, **Wageningen Marine Research** substantially contributes to more sustainable and more careful management, use and protection of natural riches in marine, coastal and freshwater areas.

Wageningen Marine Research is part of Wageningen University & Research. Wageningen University & Research is the collaboration between Wageningen University and the Wageningen Research Foundation and its mission is: 'To explore the potential for improving the quality of life'